# Model Experiments of the Conditions Generating Resonant Deep Scour

Toshihito TOYABE,Yasuharu WATANABE and Yasuyuki SHIMIZU
River Hydraulics Section
Civil Engineering Research Institute
Hokkaido Development Bureau, Japan

Kazuyoshi HASEGAWA and Kensaku NAKAMURA
Department of Technology
Hokkaido University, Japan

**Abstract**

Recently rivers are playing increasingly an important role for various purposes. Increased consciousness of the environmental impact to river areas necessitates proper planning and construction of river structures. There is a need for river planning and design of structures that can cope with different characteristics of the river banks caused by river channel shapes. This study, using data obtained from hydraulic model experiments, describes characteristics of bed topography and suggests plannning measures for river-planning and design of river establishments.

## INTRODUCTION

River bed forms depend mainly on the shape of river channels and medium-sized sand bars on the river beds. Recent theoretical studies[1)2)] and investigations[3)] using numerical simulations have established a resonance phenomenon between the shape of river channels and medium-sized sand bars, but model experiments have not investigated resonance phenomena systematically, and much is yet to be learned. The main reason for scour of river beds may be more related to resonance phenomena than is generally considered. An understanding of the conditions causing resonance phenomena in rivers is very important for flood control and when considering scour depths of river structures. This study was carried out to investigate resonance phenomena of river shapes and sand bars in river beds using hydraulic experiments with a movable bed. The results of the experiments enable a description of resonance phenomena under specific hydraulic conditions and verify existing theoretical research. The data is organized in diagrams for the design of revetments and base protection.

## OUTLINE OF EXPERIMENTS

### Objectives of Experiments

River bed forms mainly depend on curves in river channels and sand bar formation. There have been a number of studies on the formation of sand bars and domain diagrams (single row, double row) have been produced. The proposed results, like those by Kuroki, Kishi et al.,[4)] have been supported by much experimental and observational data. Kinoshita and Miwa[5)] reported that sand bar movement was dominated by the angle of meander, and that it stopped at a limiting angle. However much is left for further investigation. Except for the relations between movement limitations on sand bars and the angle of meander, other parameters as the wavelength of meander, the ratio of river-width to water depth, and the ratio of river-width to radius of curvature, are still unknown. There has been no systematic investigation of the quantitative shape and movement characteristic of sand bars in meandering flumes.

A final objective of this study is to quantitatively establish the formation and movement of sand bars under various conditions in straight and meandering river channels, and to investigate the interaction among the various conditions mentioned above, by conducting a series of experiments.

## Setting the Experimental Conditions

The conditions investigated in this study are the river channel shape and the formation of sand bars.

The shape of the experimental flume is the Sine-generated Curve Equation (1) which Langbein-Leopold[6] proposed to generally represent rivers. Here, $\theta$ is the meander angle of the flume;

$$\theta = \theta_0 \sin\left(\frac{2\pi}{\tilde{L}}\tilde{S}\right) \qquad (1) \qquad \frac{1}{\tilde{r}} = \frac{2\pi}{\tilde{L}}\theta_0 cos\left(\frac{2\pi}{\tilde{L}}\tilde{S}\right) \qquad (2)$$

$\theta_0$ is the maximum angle of meander of the flume; $\tilde{L}$ is the wavelength of meander of the flume; and $\tilde{S}$ is the length along the center line of the flume.

Arranging (1) with the metric equation $d\tilde{S} = \tilde{r}d\ \theta$ gives $(1/\tilde{r}) = (d\ \theta\ /d\tilde{s})$, and the right side represents the differential of (1); $\tilde{r}$ is the radius of curvature of the flume.

Solving (2) for $\theta_0$ with the minimum radius of curvature $\widetilde{r_0}$ gives $\theta_0 = (\tilde{L}/2\ \pi)(1/\widetilde{r_0})$, and multiplying the denominator and numerator by 1/2 of the flume width $\tilde{B}$ gives the relational equation $\theta_0 = (\tilde{B}/\widetilde{r_0})(\tilde{L}/\tilde{B})(1/2\ \pi)$. On the right side, $(\tilde{B}/\widetilde{r_0})$ and $(\tilde{L}/\tilde{B})(1/2\ \pi)$ are defined as $\upsilon$ and $1/\lambda$. Thus, $\tilde{L}$ and $\theta_0$, representing the shape of the river channel, can be represented by the dimensionless parameter $\lambda$ and $\nu$; $\lambda$ and $\nu$ are the dimensionless wavenumber of meander and the ratio of river-width to radius of curvature.

Conventionally, theoretical studies propose the ratio of river-width to water depth $\beta = (\tilde{B}/\widetilde{D_0})$ as the dominating parameter in the formation of sand bars, where $\widetilde{D_0}$ is the average water depth.

This study focuses on three parameters $\lambda$, $\nu$, and $\beta$. To obtain typical alternating sand bars, the three parameters are determined by setting hydraulic conditions with domain diagram as done in Kuroki and Kishi[4] and Kinoshita and Miwa[5]. Figures-1 and 2 plot the experimental conditions in each domain diagram of our experiments. Cases*-2,3 and 4 are assumed to form sand bars, but case*-1 is not. Flume shapes in cases 1-* and 11-* are assumed to have moving sand bars, but in cases 5-*, 7-*, and 9-* they are not.

As the water depth of the experimental flume is small compared with the particle size of river bed materials, it is not possible to develop both medium and small sand bars. The experiments here were conducted under conditions where small sand bars form with difficulty.

Conventionally proposed domain diagrams of small sand bars are based on measured values.

This study adopted the general domain diagram represented by $\tau_* \sim \widetilde{D_0}/\widetilde{d_s}$, as in Ashida

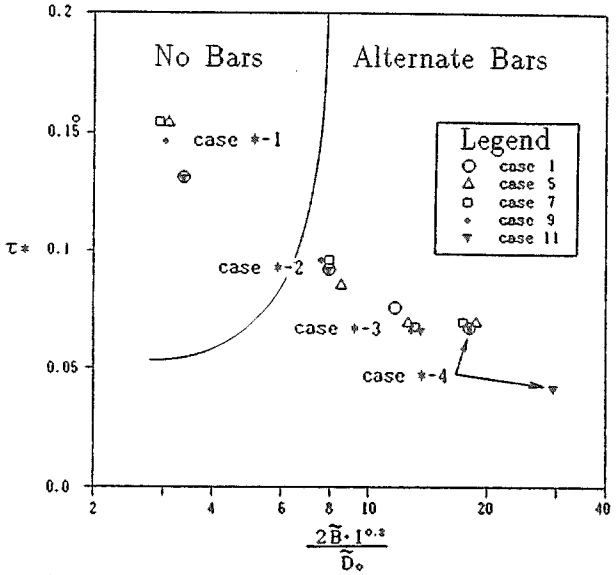


**Figure-1 Experimental Conditions with the Domain Diagram by Kuroki and Kishi**

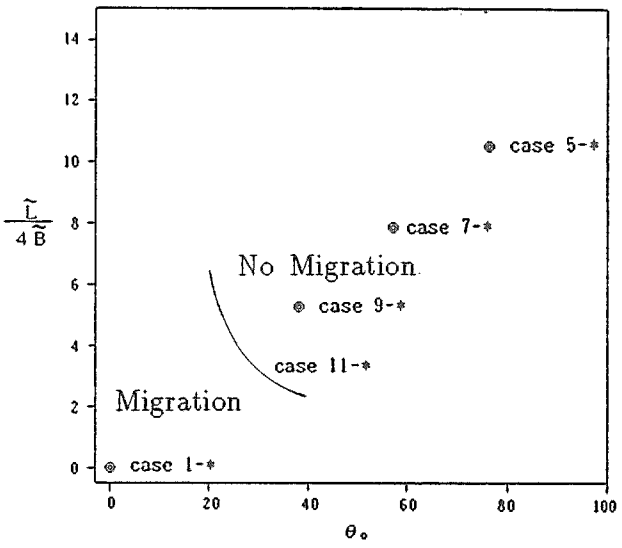


**Figure-2 Experimental Conditions with the Domain Diagram by Kinoshita and Miwa**

and Michiue et al.[7], and the drag force $\tau_*$ was set to be larger than the critical drag force $\tau_{*c}$= 0.05. Figure-3 plots these experimental conditions, and there are no cases where the lower regime caused sand ripples and dunes. Considering that flow in most parts of rivers is subcritical, the Froude number was set to be below 1. Comparing the results of experiments and the conditions of scour in the main rivers of Hokkaido, the ratio of river-width to water depth $\beta$ was set between 5 and 40, based on the conditions in actual rivers. Sufficient water depth was determined by the resistance rule of Equation (3) for cohesionless bed materials, and also to satisfy the various conditions mentioned above. Here $\widetilde{u_*}$ is the shear velocity and $\tilde{u}$ is the mean flow velocity.

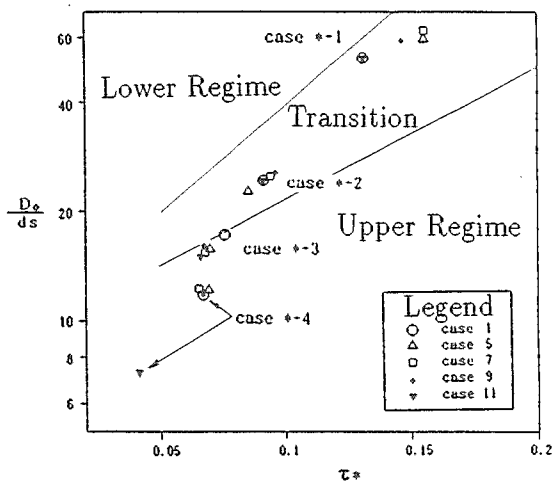


**Figure-3 Experimental Conditions with the Domain Diagram by Ashida and Michiue**

$$\frac{\widetilde{u_*^2}}{\widetilde{u_*}} = \frac{1}{\{6 + 2.5ln(\frac{\widetilde{D_0}}{2.5\tilde{d}_s})\}^2} \tag{3}$$

The flume shape and hydraulic values were set to satisfy the above conditions and to enable the amplitude to fit the size of the experimental installations. Here 20 experiments were performed using one straight flume and four meandering flumes with different $\lambda$, for four different $\beta$. Table-1 shows the particulars of the experiments. The bed material is quartz sand No.5.

Actually, the influence of the particle size of the river bed material also had to be considered, but it was disregarded in these experiments, due to the small differences in the dimensionless grain size $d_s = \widetilde{d_s}/\widetilde{D_0}$.

**Table-1 Particulars of Experiments**

| case | Meander wavelength $\widetilde{L}(cm)$ | Discharge $\widetilde{Q}(l/s)$ | Measured flume slope $I$ | Average water depth $\widetilde{D_0}(cm)$ | Bed material $\widetilde{d_s}(mm)$ | Angle of meander $\theta_0$ | $\lambda$ | $\nu$ | $\beta$ | $d_s$ | $\tau_0$ | $\eta$ |
|---|---|---|---|---|---|---|---|---|---|---|---|---|
| 01 – 1 | – | 3.97 | 1/243 | 2.96 | 0.553 | – | – | – | 5.1 | 0.019 | 0.134 | 0.255 |
| 01 – 2 | – | 1.46 | 1/161 | 1.36 | 0.553 | – | – | – | 11.0 | 0.041 | 0.093 | 1.458 |
| 01 – 3 | – | 0.79 | 1/138 | 0.96 | 0.553 | – | – | – | 15.7 | 0.058 | 0.077 | 2.477 |
| 01 – 4 | – | 0.56 | 1/106 | 0.65 | 0.553 | – | – | – | 23.1 | 0.085 | 0.068 | 3.623 |
| 05 – 1 | 628.00 | 3.99 | 1/241 | 3.33 | 0.568 | 38.217 | 0.15 | 0.10 | 4.5 | 0.017 | 0.151 | 1.545 |
| 05 – 2 | 628.00 | 1.47 | 1/161 | 1.27 | 0.568 | 38.217 | 0.15 | 0.10 | 11.8 | 0.044 | 0.087 | 3.064 |
| 05 – 3 | 628.00 | 0.81 | 1/138 | 0.87 | 0.568 | 38.217 | 0.15 | 0.10 | 17.3 | 0.064 | 0.069 | 3.674 |
| 05 – 4 | 628.00 | 0.55 | 1/106 | 0.65 | 0.568 | 38.217 | 0.15 | 0.10 | 23.0 | 0.085 | 0.068 | 3.758 |
| 07 – 1 | 471.00 | 4.01 | 1/244 | 3.35 | 0.568 | 28.662 | 0.20 | 0.10 | 4.5 | 0.016 | 0.151 | 1.609 |
| 07 – 2 | 471.00 | 1.60 | 1/160 | 1.37 | 0.568 | 28.662 | 0.20 | 0.10 | 10.9 | 0.040 | 0.094 | 2.584 |
| 07 – 3 | 471.00 | 0.80 | 1/138 | 0.85 | 0.568 | 28.662 | 0.20 | 0.10 | 17.7 | 0.065 | 0.068 | 4.103 |
| 07 – 4 | 471.00 | 0.56 | 1/106 | 0.65 | 0.568 | 28.662 | 0.20 | 0.10 | 22.9 | 0.085 | 0.068 | 3.799 |
| 09 – 1 | 314.00 | 4.02 | 1/243 | 3.29 | 0.568 | 19.108 | 0.30 | 0.10 | 4.6 | 0.017 | 0.149 | 1.406 |
| 09 – 2 | 314.00 | 1.50 | 1/161 | 1.41 | 0.568 | 19.108 | 0.30 | 0.10 | 10.7 | 0.039 | 0.096 | 2.339 |
| 09 – 3 | 314.00 | 0.80 | 1/138 | 0.86 | 0.568 | 19.108 | 0.30 | 0.10 | 17.5 | 0.064 | 0.069 | 3.749 |
| 09 – 4 | 314.00 | 0.55 | 1/106 | 0.66 | 0.568 | 19.108 | 0.30 | 0.10 | 22.9 | 0.084 | 0.068 | 3.879 |
| 11 – 1 | 188.40 | 4.01 | 1/243 | 2.96 | 0.568 | 11.465 | 0.50 | 0.10 | 5.1 | 0.019 | 0.134 | 0.890 |
| 11 – 2 | 188.40 | 1.51 | 1/161 | 1.36 | 0.568 | 11.465 | 0.50 | 0.10 | 11.0 | 0.041 | 0.093 | 2.230 |
| 11 – 3 | 188.40 | 0.81 | 1/138 | 0.83 | 0.568 | 11.465 | 0.50 | 0.10 | 18.1 | 0.067 | 0.066 | 2.863 |
| 11 – 4 | 188.40 | 0.55 | 1/106 | 0.40 | 0.568 | 11.465 | 0.50 | 0.10 | 37.3 | 0.138 | 0.042 | 6.891 |

Experimental Installation

Figure-4 is a diagram of the experimental installation. The table is 25m long and 3m wide, with 0.3m-wide meandering and straight flumes, and sand was placed according to the design. The meandering flume was made of lauan plywood (completely waterproof, 24mm thick) cut to the shape of the flume on the table, and by fixing the 30cm-deep sidewall with a vinyl chloride plate (colorless, transparent, 5mm thick) to fit to the base shape of the flume. Supports were placed to prevent deformation of the sidewall due to the weight of sand. In addition, 2cm diameter vinyl chloride pipes were buried in the

sand to prevent deformation of the river bed form when draining water after stopping the discharge, and to promote drainage.

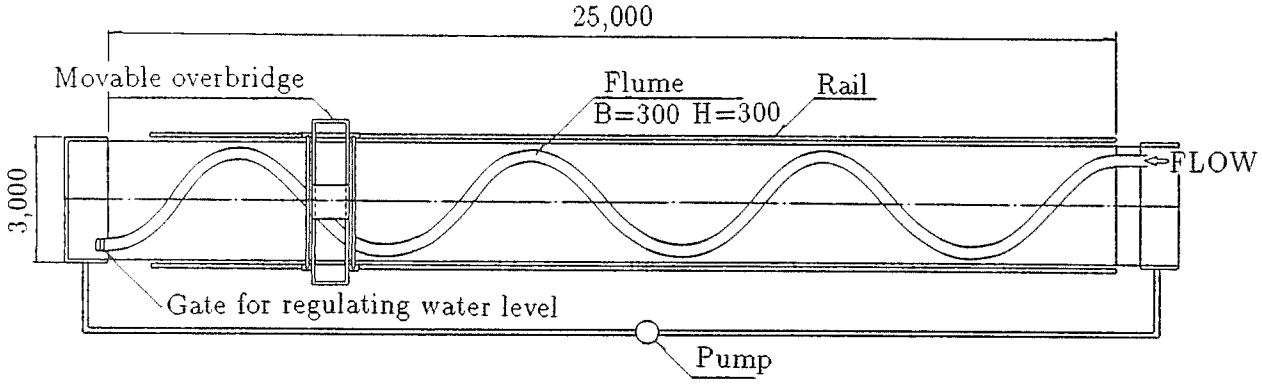


**Figure-4 Diagram of Experimental Installation**

At the start of the experiments, the flume was first flooded to prevent rapid bed variations, and then the water level and discharge were set to the design values. When the bed became stable , water levels were quickly measured. Later, water was drained, taking care not to affect the bed, and the bed height was measured after completion of the drainage. Measurements of the river bed elevation were made by an optical sensor which did not require contact with the bed.

Results

Figure-5 shows the longitudinal variations in the deepest river bed for each meander experiment. The ordinate shows the sediment amount on the average bed, which made dimensionless by dividing by the average water depth. Negative values indicate scour, and the abscissa is the downstream distance made dimensionless by dividing by 1/2 of the meander wavelength of the flume ($S$ = 0.0 is the crest of the curve in the meander flume). The average height of the river bed in each cross section is also added. In Case*-1, without sand bars, scour tends to be large at the curve crest, and small where the curve turns. This shows that river bed forms are affected by the shape of flume. In experiments with sand bars, like cases-9, -2, -3, and -4 and 7-2, and -3 where sand bars are fixed and the wavelength of sand bars and meander of the flume are really equal, river bed forms also depend on the meander shape. In case 11-2, -3, and -4, 7-4, and cases 5-2, -3, and -4, where the wavelengths of sand bars and meander are different, scour tends to be large at the top of curves, but is independent of the meander shape. In cases 5-2, -3, and -4, sand bars were expected to remain fixed as in Figure-3, but movement did take place. This supports research by Shimizu et al.[3] that movement of sand bars depends on the wavelength as well as the angle of meandering.

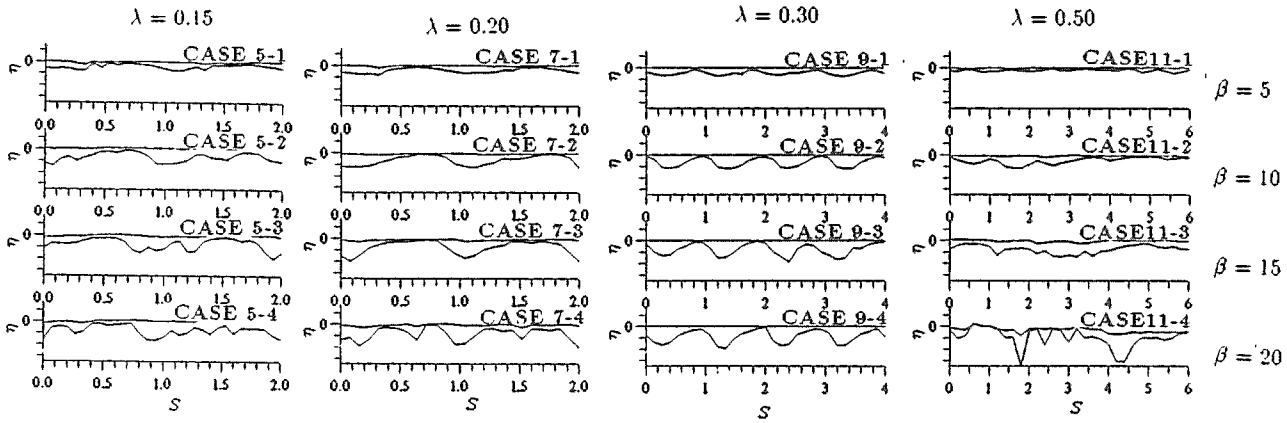


**Figure-5 Longitudinal Bed Variations of the Maximum Height in Each Experiment**

The following outlines the results of the experiments for typical cases with contour diagrams of the river bed.

Figure-6 shows contour charts of the bed for case 11, which bed the shortest meander wavelength, with (case 11-2) and without (case 11-1) sand bars. Case 11-1 without sand bars showed straight flows, sedimentation on the concave bank, erosion on the convex bank, and a dimensionless maximum depth of scour of 0.89, nearly equal to the water depth. In case 11-2, with sand bars and the same meander shape, formation of sand bars causes meandering, and the deepest bed developed at the front of bars. The wavelengths of bars and meander are different, and scour and sedimentation is independent of the shape of the flume. When the meander length is short and sand bars do not develop, scour and sedimentation occurs in places different from those generally expected.

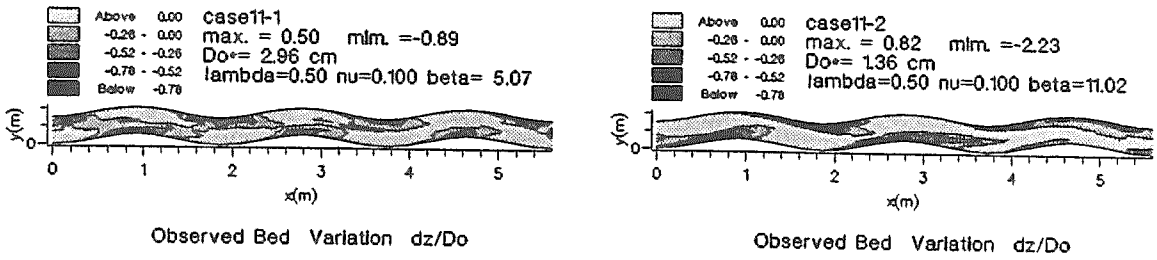


**Figure-6 Contour Charts of River Beds in Case 11-1 and 11-2**

Figure-7 shows contour charts of the experiments with (case 9-4) and without (case 9-1) sand bars. In case 9 the wavelengths of meanders and sand bars are equal. Both cases show similar river bed forms. The dimensionless maximum depth of scour in case 9-1 is 1.4 times the water depth, and in case 9-4 it is four times the water depth. It was established that much scour occurs when the wavelengths of sand bars and meanders are equal.

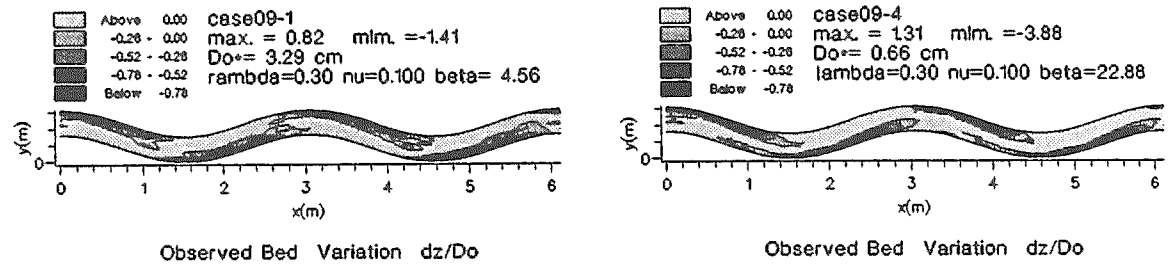


**Figure-7 Contour Charts of River Beds in Cases 9-1 and 9-4**

Figure-8 shows the results of experiments with different dimensionless wavenumbers of meander $\lambda$ for the same $\beta$ parameter of sand bar formation. Case 7-3 has a short meander wavelength, and case 5-3 has a long wavelength. Case 7-3 indicates that movement of sand bars does not correspond to the meander of the flume. Case 5-3 shows that movement of bars takes place between inflection points of a meander. Sand bars trailing away from the inflection point vanish upstream of the top of the curve, and new sand bars extend downstream, and this behavior is repeated. In this case, two pairs of alternating bars occurred for one meander wavelength, and the wavelengths of meander and sand bars were different. Figure-2 indicates that bars should not move in any of the experiments, but movement of bars was observed in case 5-3 with the longest meander wavelength. In the movement of sand bars, it is necessary to consider the relation between wavelengths of sand bars and meandering, as well as the meandering angle of the flume.

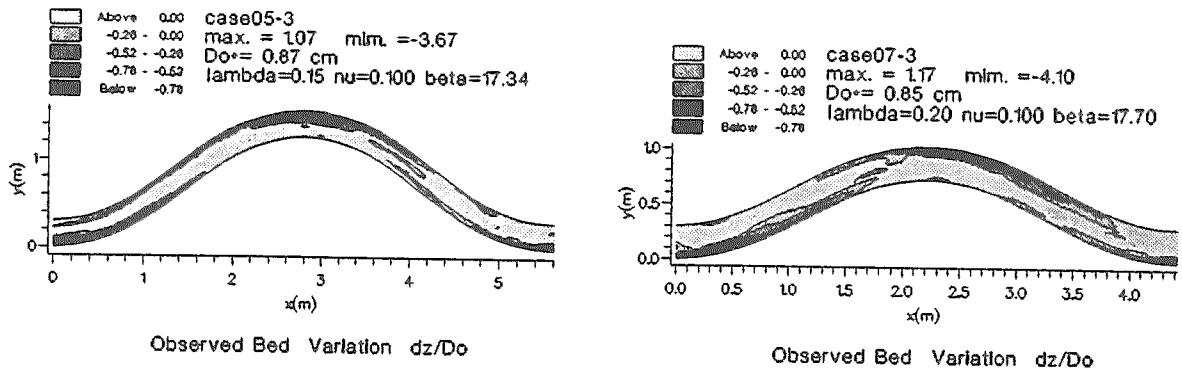


Figure-8 Contour Chart of River Beds in Cases 5-3 and 7-3

## SIZE AND PLACE OF SCOUR OF RIVER BEDS

In revetment design, it is necessary to determine the depth of penetration of the structure beneath the river bed or embarkment to prevent damage in order to from scour. thus, the possible depth of scour must be determined. An effective arrangement is also needed to preserve the ecosystem and establish water-access, as has been advocated recently. Here, the establishment of position and amount of maximum bed scour focuses on meandering river channels with sand bars.

Amount of Bed Scour

Figure-9 shows the relations between the maximum dimensionless depth of bed scour, $\eta$, and the ratio of river-width to water depth, $\beta$, for differing dimensionless wavenumbers. It indicates that $\eta$ increases with $\beta$ for all $\lambda$, and that the depth of bed scour depends largely on $\beta$, the dominating parameter of sand bar formation. Figure-10 shows the relations between the maximum dimensionless depth of bed scour, $\eta$, and the dimensionless meander wavenumber, $\lambda$, by interpolating from the values in Figure-9 for different $\beta$. For every $\beta$ value, the plotted $\eta$ indicates a maximum between 0.15 and 0.30 $\lambda$, and that it moves upward in parallel as $\beta$ increases. In the experiments with $\lambda$ between 0.15 and 0.30, the wavelength of sand bars agrees with the meander wavelength of the flume, which is considered the condition causing resonance between sand bars and the shape of flume. That is, the experiments corroborate previous investigations[1)2)3)] that the maximum scour depth increases in the domain of resonance of sand bars and shape of flume.

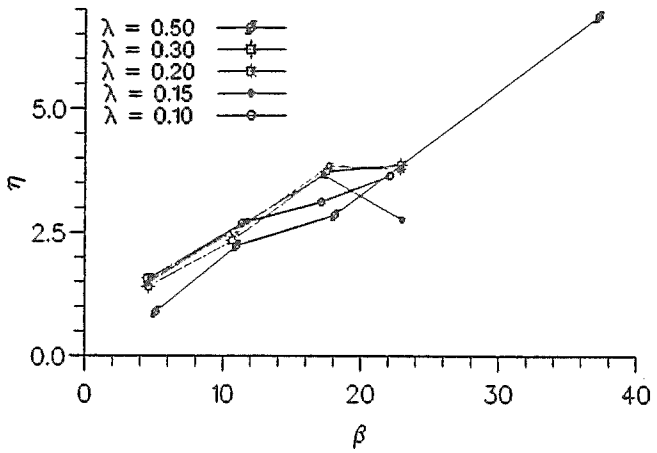


Figure-9 The Relation between the Maximum Dimensionless Depth of Bed Scour & β

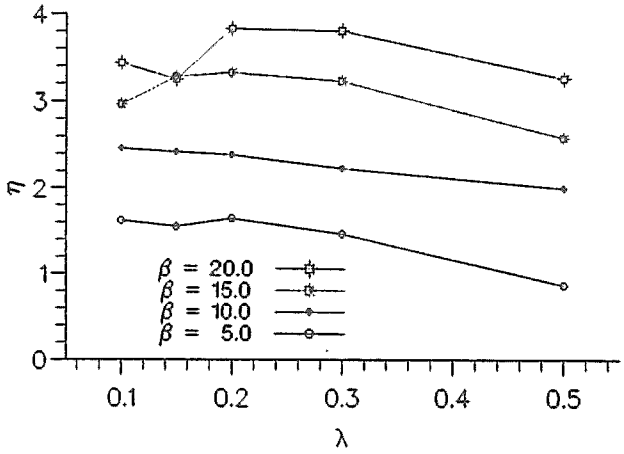


Figure-10 The Relation between the Maximum Dimensionless Depth of Bed Scour & λ

Position of Maximum Scour

Figure-11 shows where the maximum scour depth for one wavelength of each meander changes with time by expressing time after the start of the experiment as the ordinate and the dimensionless phase difference $\delta$ as the abscissa ( $\delta$ is given by making the distance from the concave bank of the top of the curve of the meandering flume to the maximum height of river bed dimensionless by dividing by 1/2 of the meander wavelength, where upstream is positive.) The maximum scour depths developing at the concave and convex banks of the top of the curve of the flume provide the dimensionless phase differences of 0 and 1. In cases 9-2,-3, and -4, and 7-2,-3, and -4 with fixed bars, the deepest river bed with one wavelength per meander develops in a specific phase. Cases 5-1, 7-1, 9-1, and 11-1 without sand bars, and 11-2, -3, and -4 with movement of bars, show that the deepest bed did not form at a fixed place but that it may occur anywhere in the bed. In cases 5-2, -3, and -4 with movement of sand bars, movement of the position of scour due to sand bars does not appear in the figure because of the large amount of scour around the top of the meander curve. This may be because the influence of the meander is larger than that of bars. For example, case 5-1 with the same dimensionless wavenumber of meandering and no sand bar indicates that the deepest river bed occurs at a specific position, though other cases without bars show it to develop in different positions. These results indicate that in cases with the same ratio of river-width to radius of curvature, river bed forms are possibly more dominated by sand bars than by the meander shape of the flume, as the dimensionless wavenumber of meandering increases. Further investigation will be necessary to verify this.

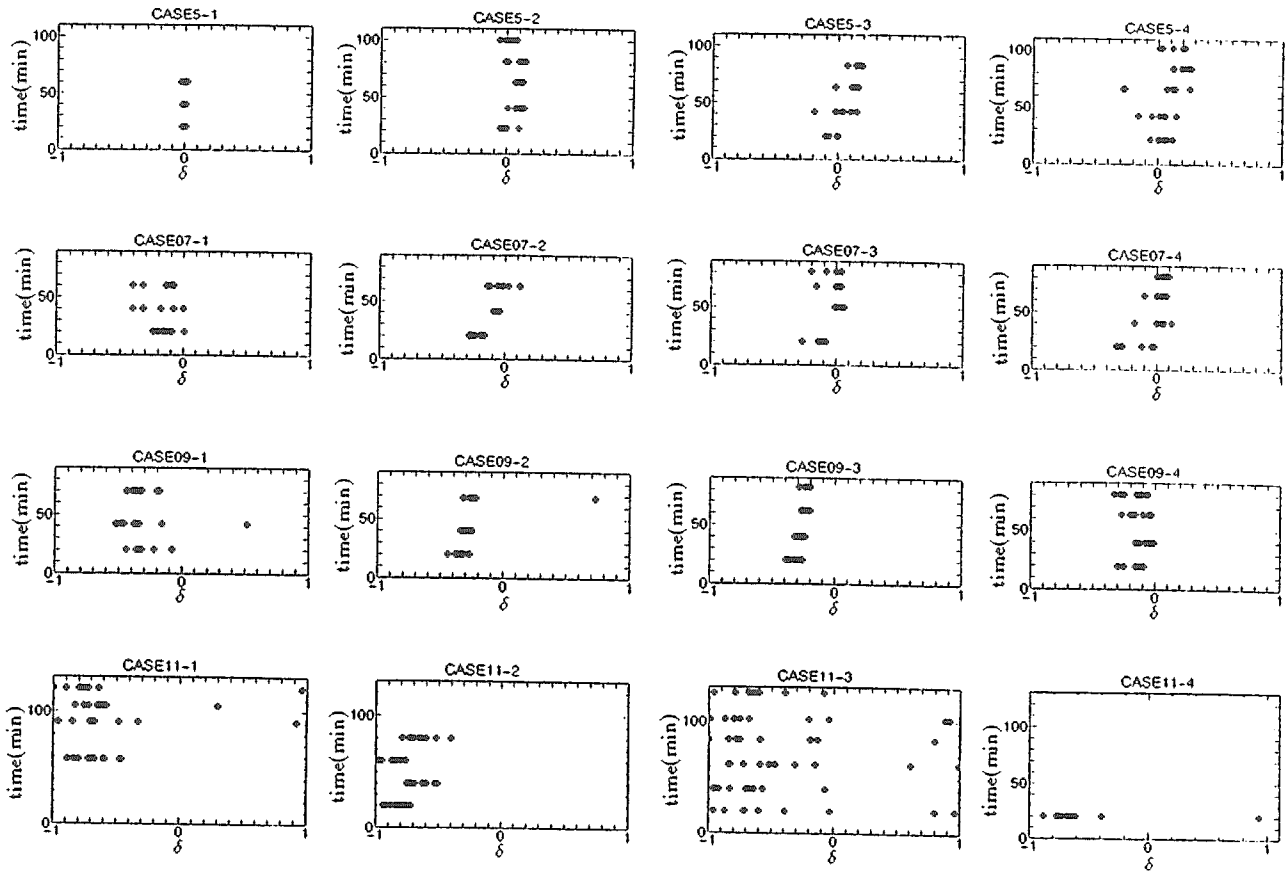


**Figure-11 Variation in Dimensionless Phase Differences with Time**

## EVALUATION OF THE DOUBLE FOURIER TRANSFORM

The double Fourier transform was used to evaluate the bed topography along the entire channel length. Figure-12 shows the dimensionless amplitude for each wave number. The double Fourier transform was calculated by;

$$\eta = \Sigma\ \Sigma\ A_{ij} sin\left(\frac{2\pi i}{4\tilde{B}}\tilde{n} - \frac{\pi}{2}\delta_{ie}\right) cos\left(\frac{2\pi i}{\tilde{L}}\left(\tilde{S} - \sigma_{ij}\right)\right) \tag{4}$$

$\tilde{S}$, $\tilde{n}$ = longitudinal and stream wise coordinate, respectively, $\sigma$ is the abscissa and $\delta_{ie} = (1 + (-1)^i)/2$. The wave number i=1 corresponds to double the flume width, and the wave number j=1 corresponds to the length of one meander."A" is the dimensionless amplitude of each wave number (dimensionalized by the average water depth). According to Hasegawa[8], alternating sand bar shapes and meandering river shapes can be well expressed by the low frequency waves such as (1,1),(2,0),(3,1),(2,2). In each case, the wave (1,1) shows a high value. In cases 5,7, and 9, the amplitude of wave (1,1) is between 0.8 and 1.0 under conditions with or without sand bars. However case 11 whose meandering wavelength is shorter then case 5,7 , and 9, shows a low value for (1,1). The value of the wave (2,0), (3,1) and (2,2) are high in this experiment. There was little correlation between the waves (2,0),(3,1) and "$\beta$". Wave (2,2), tended to have a larger amplitude with the increase of "$\beta$". On the other hand, this wave has a low amplitude when there are no sand bars. Thus, when sand waves appear,these waves tend to increase their amplitude. This fact is in accordance with Hasegawa's study.

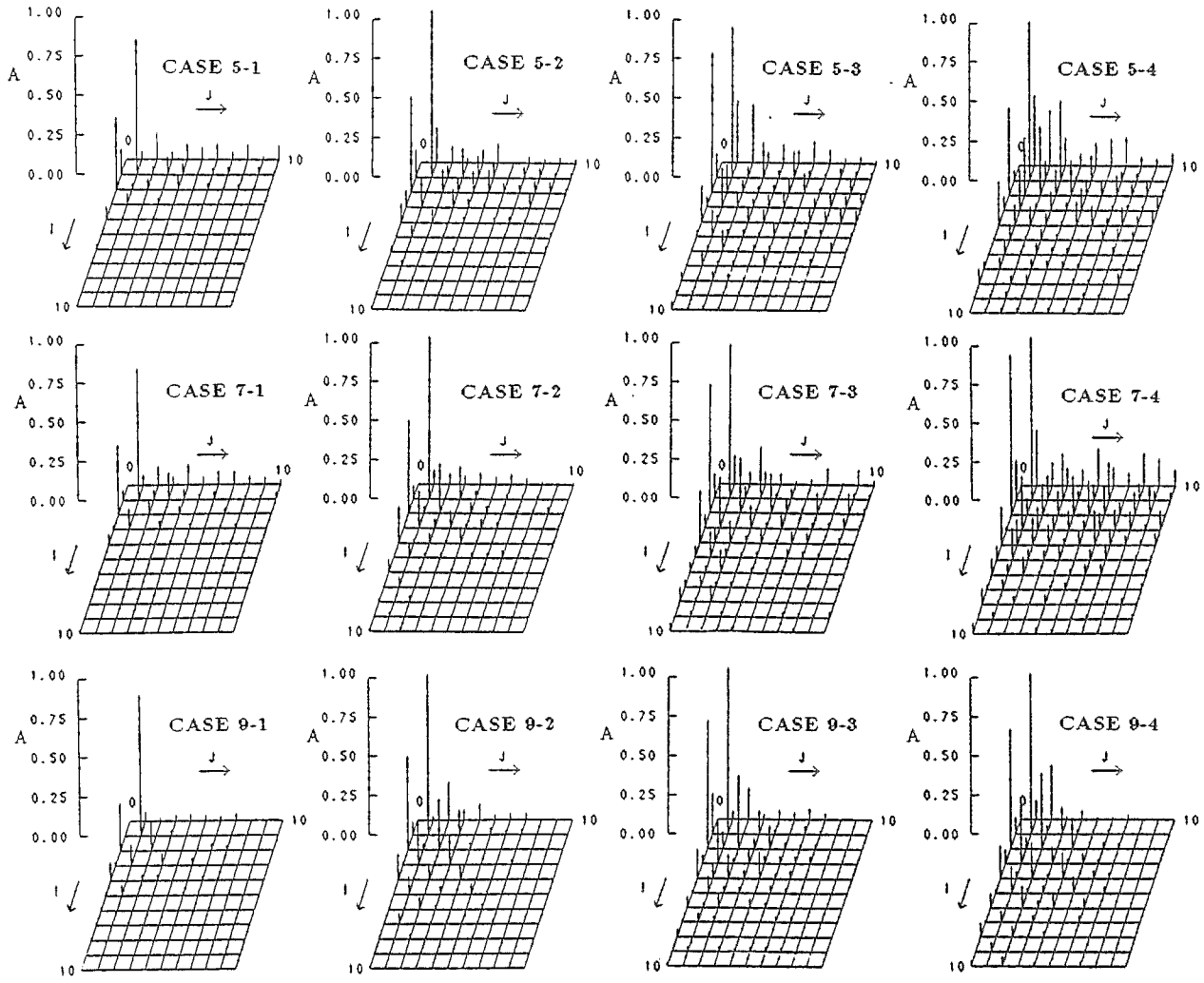

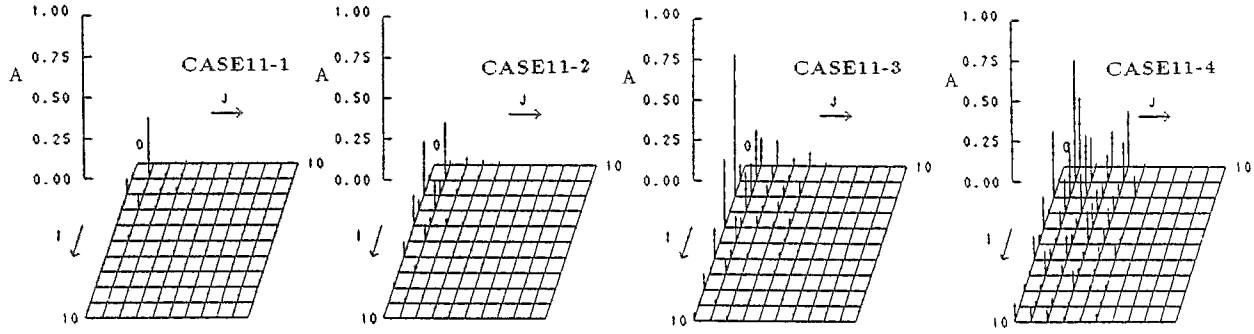


**Figure-12 Dimensionless Amplitude Versus Wave Number**

## Summary

Experiments were performed on the resonance between sand bars and meanders of flumes, and the results are:

1) Movement and disappearance of sand bars are affected by the meandering angle of the flume and the relation between the wavelengths of sand bars and meanders.

2) Large scour develops when both sand bars and meanders are present.

3) The dimensionless maximum depth of scour increases with the ratio of river-width to water depth, $\beta$, and reaches a maximum value at a specific dimensionless meander wavenumber, $\lambda$.

4) At the same ratio of river-width to radius of curvature, river bed forms are more affected by sand bars than by the meandering shape of the flume. This is increasingly true when the dimensionless meander wavenumber increases.

5) The amplitude of wave (1,1) is between 0.8 and 1.0 in the range $\lambda$ =0.15 - 0.3 regardless of the appearance of sand bars. Outside of this range, the amplitude is low.

6) The amplitude of waves (2,0) and (3,1) show high values in the sand bar experiment. In the experiment without sand bars it was low.

7) The amplitude of wave (2,2) is also high in the sand bar experiment and has the tendency to inerease with an increase of "$\beta$".

Further investigation is necessary to establish the conditions of resonance in order to pedict the maximum scour of the river bed and the details of bar formation. Further experiments are also needed with different $\nu$ and ds values.

## REFERENCES

1)Blondeaux, P. and Seminara, G.(1985) "A Unified Bar-bend Theory of River Meanders", Journal of Fluid mechanics,No.157.

2)Parker, G. and Johannesson, H.(1989) "Observation on Several Recent Theories of Resonance and Overdeepening, River Meandering", AGU Monograph, No.12.

3)Shimizu,Yasuyuki.,Tubino,Marco and Watanabe,Yasuharu.(1992) "Numerical Analysis of River Bed Variations under Resonance Conditions with Free and Alternating Sand Bars", Collection of Papers of Hydraulics, Vol. 36.

4)Kuroki,Mikio and Kishi,Chikara.(1984) "A Theoretical Study of Domain Classification of Medium-sized River Bed Forms",Papers Collection of the Society of Civil Engineering,No.342.

5)Kinoshita,Ryosaku and Miwa,Hitoshi.(1974) "The Shape of River Channels with Stable Alternating bars",29th Annual Scientific Lecture Meeting of the Civil Engineering Society.

6)Leopold, L.B. and Wolman.M.G.(1957) "River Channels Patterns, Braided, Meandering and Straight", Geological Survey Professional Paper, 282-B.

7)Ashida,Kazuo and Michiue,Masanori.(1972) "A Study of Resistance and Bed Load of Movable Bed Flows",Collection of Papers and Reports of the Civil Engineering Society, No.206.

8)Hasegawa,Kazuyoshi.(1984) "Hydraulic research on planimetric forms, Bed Topographies and flow in alluvial rivers",Dissertation presented to the Hokkaido Unversity, at Sapporo, Japan, in partial fultillment of the requirements for the degree of Doctor of Philosophy.

9)Nakamura,K. Hasegawa,K. Shimizu,Y Watanabe,Y Toyabe,T.(1992) "Harmonic Analysis on free and forced bar forms in experimental meandering cahnnels with resonance condition",Papers Collection of the Civel Engineering Branch Society, No.49.